A model of immune regulation as a consequence of randomized lymphocyte division and death times

E. D. Hawkins*[†], M. L. Turner*[†], M. R. Dowling*[‡], C. van Gend*, and P. D. Hodgkin*[§]

*Immunology Division, The Walter and Eliza Hall Institute of Medical Research, 1G Royal Parade, Parkville, Victoria 3050, Australia; [†]Department of Medical Biology, University of Melbourne, Parkville, Victoria 3010, Australia; and [‡]School of Physical Sciences, University of Queensland, Queensland 4072, Australia

The magnitude of an adaptive immune response is controlled by the interplay of lymphocyte quiescence, proliferation, and apoptosis. How lymphocytes integrate receptor-mediated signals influencing these cell fates is a fundamental question for understanding this complex system. We examined how lymphocytes interleave times to divide and die to develop a mathematical model of lymphocyte growth regulation. This model provides a powerful method for fitting and analyzing fluorescent division tracking data and reveals how summing receptor-mediated kinetic changes can modify the immune response progressively from rapid tolerance induction to strong immunity. An important consequence of our results is that intrinsic variability in otherwise identical cells, usually dismissed as noise, may have evolved to be an essential feature of immune regulation.

Intermitotic times of yeast, protozoan, and mammalian cells can vary broadly, with little, if any, inheritance of division time from parent cells (1–6) [Note 1 in supporting information (SI) *Text*]. The bulk of this variability is observed in the G_1 phase of cell cycle (2). We have also noted broad variation in times to first division by resting murine and human lymphocytes (7, 8) *in vitro*. This variation conforms to a lognormal distribution consistent with a stochastic process affecting times to divide. It is not clear as yet whether variability arises internally within identical cells or as the result of a history of variable exposure of identical cells to external influences. Irrespective of its genesis, this variability in time to first division is the primary source of cell division heterogeneity in populations, as revealed by fluorescent division tracking methods (7, 9). T and B lymphocytes typically take between 30 and 50 h to enter their first division and then take ≈9 h to passage through each subsequent division round (9). As a consequence of variation in the first division time, the dividing cells are found spread over three to five consecutive division numbers as they progress (9). Relatively simple models of growth developed within this framework have been used to extract division and death rates from time series data and provide novel insights into how receptor-delivered signals regulate lymphocyte growth (7, 9). Furthermore, mathematical models based on the Smith–Martin concept of two phases of the cell cycle have been successfully applied to division tracking data (10–14). Despite this success, we are interested in developing more accurate models that include experimentally validated rules for how cells interleave times to division and times to die and how they are inherited from one generation to the next. To explore these questions, we used B lymphocytes as our experimental model because of their sensitivity to signals affecting both growth and survival *in vitro*. Here, we propose a general model of cell growth regulation that is suitable for robustly fitting division tracking data. Furthermore, we use our model to illustrate that variability in times to divide and die can be an essential property of lymphocytes that enables exquisite quantitative regulation of the strength of the immune response.

Results

Times to Die and Divide: First Division. When naive T or B lymphocytes are purified from lymphoid tissue and placed in tissue culture without stimulation, they progressively die by apoptosis, apparently because of removal from homeostatic survival signals *in vivo* (9, 15).

When first examined, cell loss seemed to follow an exponential decay function consistent with a constant probability of dying over time (Fig. 1A and refs. 7, 9, and 15). However, we noted deviations from the exponential when more time points were measured (Fig. 1 A and B). These deviations fell into two classes. In many experiments there was a rapid loss of cells over the first 6 h, before viability stabilized. This loss was affected by the manner of preparing cells; B cells prepared quickly showed little initial loss (Fig. 1B). The second pattern of death is seen clearly in Fig. 1B where a lag is followed by a gradual loss of cells over time. A similar pattern of cell loss is seen in Fig. 1A once the rapid, early death is considered. Because we have frequently observed lognormal distributions in relation to times taken for cells to divide (7, 8), we hypothesized a lognormal time to die curve, as shown in Fig. 1B. This hypothesis fit the data for cell loss extremely well (Fig. 1A). Other density functions with similar long-tail characteristics were fitted. Typically the two-parameter skew distributions, lognormal, gamma, and Weibull all gave excellent fits and each may find application in different situations (Note 2 in *SI Text*). IL-4 modulates B cell viability without stimulating cell growth by means of the up-regulation of the anti-apoptotic molecule Bcl-xl (16–18). This efect is shown in Fig. 1C. A lognormal density function also fits the loss of B cells cultured with varying concentrations of IL-4 (Fig. 1C) (Note 3 in *SI Text*). Interestingly, increasing IL-4 concentration increased the mean time to die but not the value for the variance (Fig. 1D). We conclude that time to death is capable of being programmed for a particular mean time and altered by signals such as IL-4. Further evidence that the time of death follows an age-dependent distribution, rather than the age-independent exponential, was noted by modulating the crucial survival proteins Bim and Bcl-2 (19, 20). The survival curves of B cells from Bim-deficient or Bcl-2-overexpressing mice are well described by a lognormal distribution, but the mean times to die are extended to 81 h and 234 h, respectively (SI Fig. 6). These results illustrate that the expression of antiapoptotic molecules contributes to the setting of the mean time to death, rather than controlling a constant probability of dying over time.

Independent Control of Survival and Division. When resting T and B cells are polyclonally stimulated *in vitro* the time taken to enter into the first round of division is longer than for subsequent divisions (9) and can be varied by the stimulation conditions. This result can be visualized experimentally by arresting cells in G_2/M of their first
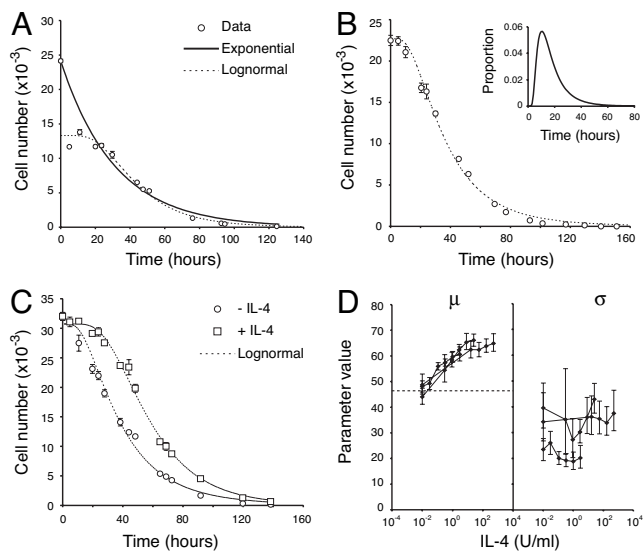
Fig. 1. Probabilistic regulation of time to die. Small resting B cells from spleens or lymph nodes were placed in culture under different conditions, and survival was measured by propidium iodide uptake. Cell numbers were counted by reference to beads as described (7). Fitting was performed by using a Matlab fmincon function. (*A*) Survival curves were fitted by using an exponential decay function [solid line, $k = 0.35$, 95% confidence interval (C.I.) (+0.011, −0.008)] or a lognormal survival function without $T = 0$ and $T = 1$ [dashed line, $\mu = 48.55$, 95% C.I. (+2.3, 2.2), $\sigma = 24.90$, 95% C.I. (+4.6, −4.5)]. (*B*) Survival of B cells isolated from lymph nodes by using the quick preparation method. Data fitted using lognormal survival function [dashed line, $\mu = 42.59$, 95% C.I. (+4.6, −4.5), $\sigma = 29.08$, 95% C.I. (+3.8, −3.0)]. The probability distribution function of the fitted lognormal is represented in *Inset*. (*C*) Survival curves of B cells isolated from spleen and cultured either alone [circles, $\mu = 45.40$, 95% C.I. (+1.8, −1.7), $\sigma = 36.94$, 95% C.I. (+7.3, −5.9)] or with saturating IL-4 [squares, $\mu = 62.33$, 95% C.I. (+2.2, −2.0), $\sigma = 30.02$, 95% C.I. (+5.1, −4.2)]. (*D*) The values for μ and σ of lognormal survival function fit to viability data for three experiments titrating IL-4. Error bars for *A–C* represent SEM for triplicate samples. Error bars in *D* represent 95% C.I.s assigned by using a Monte Carlo simulation.

Fig. 2. Independent times to die and divide. Resting B cells were placed in culture with 10 μg/ml, 3.3 μg/ml, or 0 μg/ml α-CD40 and 500 units/ml IL-4. (*A*) B cells were cultured in the presence of colcemid, and a time course of 1 h [³H]thymidine pulses was conducted. Cells were harvested and scintillation counted. Lowering α-CD40 concentration delayed μ [60.53, 95% C.I. (+1.1, −1.3) vs. 73.56, 95% C.I. (+3.1, −2.6)] and increased σ [19.01, 95% C.I. (+1.8, −2.5) vs. 24.89, 95% C.I. (+4.9, −4.0)]. (*B*) B cell number was measured by flow cytometry by using the protocol described in ref. 7. After 48 h, cell numbers increased in a dose-dependent manner. Before 48 h, cell numbers remained the same regardless of stimulation level. (*C*) The independent operation of times to divide and times to die for B cells stimulated with 10 μg/ml α-CD40 and 500 units/ml IL-4 is represented here by a cyton plot. The times to divide and times to die are represented as positive and negative values, respectively. Assigning probability distributions to the variations in times to divide and die allows the number of cells dividing and dying in each time interval to be quantitated. The net effect of the two independent timed events is shown in the shaded area.

division. The mean time to divide varies with stimulus concentration, illustrating the wide spectrum of time modulation that is possible (Fig. 2*A*). The broad variation in times to divide revealed by this method is characteristic for all systems studied so far and is well fitted by a lognormal in each case (Fig. 2*A* and refs. 7 and 8).

Lymphocytes placed in culture with a polyclonal stimulus are subject to conflicting motivations to die or divide, and each can be regulated by extrinsic signals. An important question for modeling the net result is how the two mutually exclusive outcomes are resolved within a cell. It has been reported that T cell activation with αCD3 does not alter the rate of loss of cells for a number of days (7). This pattern can also be seen for B cells stimulated with α-CD40 and IL-4 (Fig. 2*B*). The rate of death of cells is not affected in the period before the time at which the surviving cells begin dividing. Our hypothesis to explain this result is the independence of the survival and division machinery inside each cell (7, 9). Each cell placed in culture has a time to die and each mitogenic stimulus activates the cells and imposes a time to divide that also varies in the population according to a lognormal distribution. The two timed processes within the cell are unaware of each other and whichever outcome is reached first determines the fate of that cell. This cellular 'machinery' is illustrated in SI Fig. 7 for individual cells. Fig. 2*C* gives an example of the calculation of net cell numbers. The combination of independent cellular machines governing times to divide and die therefore represents a key regulatory unit of the cell (Note 4 in *SI Text*). We propose the name cyton for this unit. To represent a cyton we plot time to divide as a positive probability and
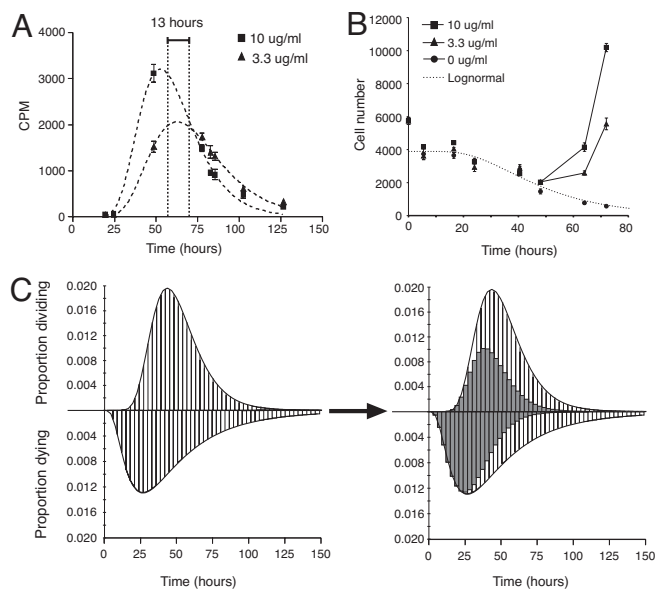
time to die as a negative (Fig. 2*C*). Similarly, we can represent a cyton symbolically using two probability distributions ϕ and ψ as

$$
\left| \begin{array}{c} \phi(\dots) \\ \psi(\dots) \end{array} \right| \qquad [1]
$$

with ϕ representing time to divide and ψ time to die, whereas (…) stands for the required parameter values. A cyton can operate with any probability distribution, but we find the lognormal probability density function is an excellent representation of experimental data and we use it here to illustrate our argument for both division time and death time (Note 5 in *SI Text*). Given parameter values for the distributions of time to die and divide and the starting cell number (*N*), the number of cells dividing or dying per unit time at time t can be calculated:

$$
n^{div}(t) = N\left(1 - \int_0^t \psi(t')dt'\right)\phi(t), \qquad [2]
$$

$$
n^{die}(t) = N\left(1 - \int_0^t \phi(t')dt'\right)\psi(t). \qquad [3]
$$

The factors in parentheses account for the cells that would have divided at time t but had previously died, and vice versa, respec-

tively. The independent action of death and division thus reduces the initial pool of cells available for the other process as time progresses. This calculation is illustrated in Fig. 2C (Note 6 in *SI Text*).

Generalized Cyton Model. The above probabilistic calculation delivers the number of cells that enter division over time. However, to develop a model that can predict the number of cells in each division at any time we must account for the fate of cells after they divide the first time. Lymphocytes typically progress through a series of division rounds much more quickly than they took to enter the first division. Furthermore, the intermitotic times through subsequent divisions are not affected by the time taken to reach first division (9, 21). BrdU labeling also indicates that average division times are not shorter among cells that have reached later divisions (7, 9, 21). Thus, there is no evidence as yet for a significant inheritance of division times by lymphocytes, as has been noted in studies of mother-daughter inheritance (1, 3, 22) and for inheritance of key growth factor receptors by T cells (1).

Based on the lack of inheritance of division times noted for dividing lymphocytes we propose that general cell proliferation obeys the following rules:

1. The operation of the regulable cyton controlling division and survival, seen leading up to the first division, is repeated through subsequent divisions.
2. Individual cells will, upon division, "erase" the values of the parents for times to divide and die, and adopt new values drawn from the appropriate distribution.

Thus we can assign a cyton term for each division:

$$\left\lfloor \begin{array}{c} \phi_0(\ldots) \\ \psi_0(\ldots) \end{array} \right\rfloor_0 \left\lVert \begin{array}{c} \phi_1(\ldots) \\ \psi_1(\ldots) \end{array} \right\rVert_1 \ldots \left\lVert \begin{array}{c} \phi_m(\ldots) \\ \psi_m(\ldots) \end{array} \right\rfloor_m, \quad [4]$$

where m is the largest division class being analyzed [typically m is ≈ 8 in current carboxyfluorescein diacetate-succinimidyl ester (CFSE) experiments because of technical limitations]. Given probability densities ϕ and ψ_i, $i = 0, 1, \ldots, m$, which might each be specified by a small number of parameters, the above cyton expression can be solved to yield the number of cells that divide or die in each division class at any time, as well as the cumulative number of cells in each class. As such the solution will allow comparisons to experimental data and evaluation of the underlying assumptions.

The formulae in Eqs. **2** and **3** apply to the activation of an homogeneous cell population where all cells will eventually divide if they do not die first (Note 7 in *SI Text*). However, in reality not all cells in a population will eventually divide if they avoid death. Some may be nonresponsive to the stimulation, for example through the lack of an effective receptor (23). Alternatively cells may clearly respond, as evidenced by cell size increases or expression of activation markers, but not go on to divide (7). Thus, we introduce the parameter progressor fraction, pF_0, the proportion of the population that will divide in response to the stimulation. This factor modifies the formulae in Eqs. **2** and **3** to give the following expressions for the number of cells dividing for the first time or dying to exit division class 0 (Note 8 in *SI Text*)

$$n_0^{div}(t) = pF_0 \cdot N \cdot \left(1 - \int_0^t \psi(t')dt'\right) \cdot \phi(t), \quad [5]$$

$$n_0^{die}(t) = N \cdot \left(1 - pF_0 \cdot \int_0^t \phi(t')dt'\right) \cdot \psi(t). \quad [6]$$

For division classes $i = 1, 2, \ldots, m$, the number of cells dividing or dying per unit time at time t are given by

$$n_i^{div}(t) = 2 \cdot pF_i \cdot \int_0^t dt' n_{i-1}^{div}(t') \cdot \left(1 - \int_0^{t-t'} dt'' \psi_i(t'')\right) \cdot \phi_i(t - t'),$$
$$[7]$$

$$n_i^{die}(t) = 2 \cdot \int_0^t dt' n_{i-1}^{div}(t') \cdot \left(1 - pF_i \cdot \int_0^{t-t'} dt'' \phi_i(t'')\right) \cdot \psi_i(t - t'). \quad [8]$$

One can think of cells entering division class i from the previous division at different times t' as separate cohorts that divide or die as described in the previous section. The integrals in the above equation simply sum over the different starting times of these cohorts with different starting cell numbers, $2n_{i-1}^{div}(t')$, and different times to division or death, $t - t'$. In these equations we have also incorporated a progressor fraction for subsequent divisions, pF_i, to account for the possibility that some cells stop dividing at particular division classes and remain there until they die. For experimental systems under continuous stimulation, the progressor fraction for subsequent divisions after the first is practically 1, and we do not need it to obtain good fits. However, in the next section, we study systems that receive stimulation only for a limited time, in which case cells tend to stop dividing after a small number of divisions so the progressor fractions for subsequent division are <1.

To calculate total cell numbers in each division as a function of time, $N_i(t)$, the number of cells that have entered that division from the previous division over all previous times are added, and the number that have left by means of division and death are subtracted

$$N_0(t) = N - \int_0^t dt'(n_0^{div}(t') + n_0^{die}(t')), \quad [9]$$

$$N_i(t) = \int_0^t dt'(2n_{i-1}^{div}(t') - n_i^{div}(t') - n_i^{die}(t')), \quad i = 1, 2, \ldots, m.$$
$$[10]$$

Depending on the division and death distributions that define the cyton, these integrals could be evaluated to give the number of cells in each division as a function of time. This calculation can be done analytically for the case of exponential distributions (constant rates of division and death), and possibly other simple distributions. However, for most distributions an analytic solution will not exist so numerical techniques will be needed (Note 9 in *SI Text*). To this end, we developed a numerical solver [general cyton solver (GCytS)] that has the flexibility to substitute different probability density functions and parameter values for consecutive divisions. GCytS was implemented in Matlab (Mathworks, Natick, MA). The primary operation of GCytS algorithms is given in quantitative implementation method provided. Fig. 3A shows several solved examples where the probability density function chosen is lognormal and parameter values are kept constant after first division. The results illustrate how subtle changes in mean times to die and divide can vary the rate of cell expansion from rapid growth to rapid cell loss. The extreme sensitivity to small changes in parameters is emphasized by noting the 300-fold difference in cell number after 80 h that results from a simultaneous lengthening of time to divide and shortening of time to die by 20%. SI Fig. 8 illustrates the positive role variance plays in the effective operation of the cyton machinery. With little variation in times to division and death, there is a switch-like outcome yielding either a maximally strong response or a rapid loss of all cells as the mean times to divide and die are
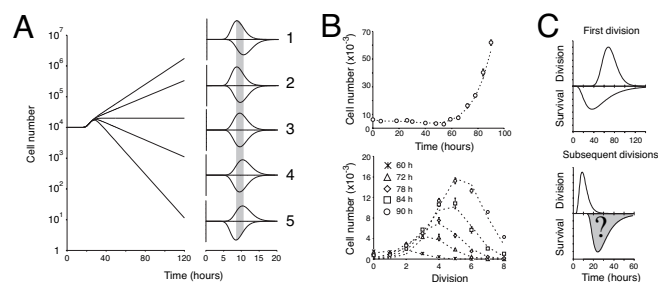
Fig. 3. The generalized cyton model. (A) Cell number over time is plotted for five different cyton configurations. Progressing from cyton plot 1 to 5, the median times to divide ($\phi_{i>0}$) and die ($\psi_{i>0}$) in subsequent divisions are increased and decreased, respectively, by <20% (represented by the shaded area in cyton plots). These subtle shifts cause a large net change in the response from expansion (trace 1) to contraction (trace 5). Cyton parameter values: trace 1, $\phi_{i>0}$ 9, $\psi_{i>0}$ 11; trace 2, $\phi_{i>0}$ 9, $\psi_{i>0}$ 10.5; trace 3, $\phi_{i>0}$ 10, $\psi_{i>0}$ 10.5; trace 4, $\phi_{i>0}$ 11, $\psi_{i>0}$ 10.5; trace 5, $\phi_{i>0}$ 11, $\psi_{i>0}$ 9. s is kept constant at 0.2 for all cyton plots. (B) B cells were labeled with CFSE and stimulated with 10 μg/ml α-CD40 and 500 units/ml IL-4. Cells were harvested at different times, and the total cell number as well as number of cells in each division was calculated. The optimal cyton solution is shown by dashed lines. Mean and SEM values of three replicates are shown. (C) Cyton solution of data shown in B. By using the data available, the cyton solution for time to death in subsequent divisions cannot be constrained.

Fig. 4. Modeling division and death. CFSE-labeled B cells were stimulated with 30 μg/ml α-CD40 and 500 units/ml IL-4, and cell numbers were followed by flow cytometry. Identical cells were washed after 40 h of stimulation and recultured either with or without stimulus. (A and B) Cell numbers per division for various harvest times during continual stimulation (A) or after stimulus removal (B) are shown. Increasing culture period before stimulus removal led to an increase in the mean division number before division stops (C, green = 30 h, blue = 40 h, red = 50 h). (D–F) Total cell numbers for 30 h (D, green), 40 h (E, blue), or 50 h (F, red) before stimulus removal. Control cultures with continual stimulation are shown in G (black). (H) The resulting division destiny distributions for each data set (colors representing stimulation time). An optimal cyton solution was determined for each data set by using the modified GCytS in which the division destiny was implemented. The value for $\phi_{i>0}$ (med = 6.27 h and s = 0.05 h) was determined from continual stimulation data and fixed for all data sets. The resulting fits to experimental data are shown by black lines in D–F. (I) The optimal values for parameter $\psi_{i>0}$ obtained for each data set (colors representing stimulation duration). The gray line for $\psi_{i>0}$ shown in I is the average value of med and s for 30-, 40-, and 50-h stimulus removal data (med = 30.1 h and s = 0.35 h). This average value for $\psi_{i>0}$ was used in an alternative cyton fit (gray lines in D–F) and was also used to fit continual stimulation data G. These model solutions illustrate that the slight variations obtained in $\psi_{i>0}$ do not appreciably affect the fit to total cell number data and that the same parameter value can apply to cells in continual stimulus. Data points represent mean and SEM of three replicates.

varied. However, as the variance of both elements of the cyton is increased the transition between rapid cell loss and growth is softened, allowing many more transitional quantitative outcomes to occur. Such a quantitative scenario is more typical of our experience of immune responses under many different conditions.

Our GCytS can calculate total cell numbers at any time after initiation of culture, the number of cells in each division, and the number of dead cells and times of death. Therefore, appropriate parameters can be found to fit experimental data from CFSE division tracking experiments that report total cell number and cells per division for both live and dead cells. GCytS was linked to optimization routines in Matlab to apply to particular data sets. In Fig. 3B, the number of B cells in each division was determined over a series of harvest times after stimulation with α-CD40 and IL-4. The optimal solution from GCytS is shown, illustrating the possible excellent fits. The cyton model fits for three independent experiments measuring proliferation under the designated conditions were compared with both a Smith–Martin model (2) and the Deenick six-parameter proliferation model (7) (Note 10 in *SI Text*). We used Akaike's information criterion (AIC) as a guide for comparison taking account of the different number of parameters used in each model (24). In all experiments the difference in AIC values (ΔAIC) between the cyton model and other proliferation models was $\geq$10 (Note 11 in *SI Text*). ΔAIC values $\geq$10 indicate that the cyton model offers a superior fit to the data despite the addition of two extra parameters (24, 25). Nevertheless, fitting to live cell numbers alone does not give an exclusive solution for subsequent division and death parameters as faster division times can to some extent be counteracted by earlier mean times to die (data not shown). The solution is well constrained if the number of dead cells per division can also be included in the data set examined by GCytS (data not shown). However, this information is difficult to obtain with the CFSE method. Thus, we explored experimental systems more dependent on death to help further validate our model.

Regulating the Number of Divisions. Stimulated lymphocytes do not divide indefinitely. However, the number of consecutive cell divisions they undergo can vary. For example α-CD40 stimulated B cells divide three to four times after stimulus is removed before they have entered their first division (26), whereas CD8 T cells divide at least eight times after stimulus removal (27, 28). Thus, stimulation
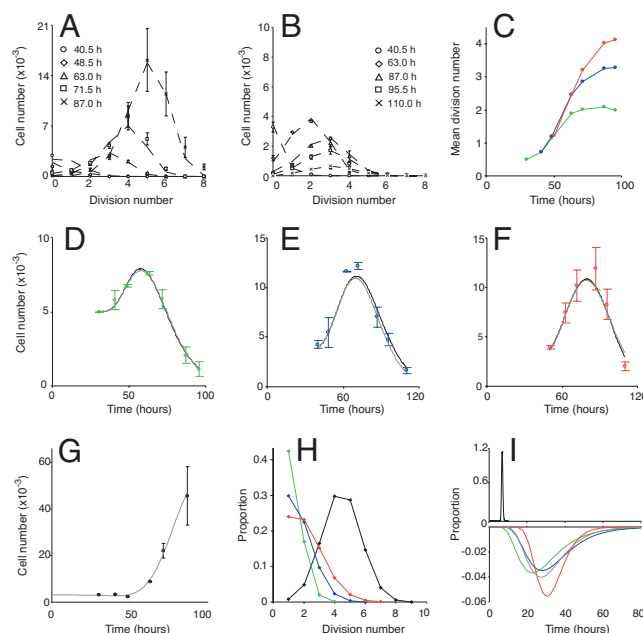
can initiate a variable number of division rounds, possibly by accumulating an excess of mitosis triggering molecules that dilute with division. When cells stop dividing they usually die rapidly (26). The cyton model can describe this behavior in a very simple and biologically intuitive manner. For a rapidly dividing population the division time of individual cells is usually shorter than the underlying time to die and the cells are thus more likely to divide; however, if the impetus to divide ends then the underlying time to death and associated variance should be revealed.

To examine the process of division cessation and test the above hypothesis, B cells were exposed to varying time periods of stimulation. When stimulus was removed after 40 h, B cells divided on average three times before dying compared with continuous stimulation in which division continued (Fig. 4 A and B). Analysis of cell division after stimulus removal at 30, 40, or 50 h revealed that increasing the duration of stimulus enables cells to progress through more divisions (Fig. 4C). These experiments illustrate that progression through division number can be regulated (26). However, quantitative analysis of the number of divisions cells undergo is complicated by the high level of death that follows once division stops. To more accurately measure cell progression, the same

IMMUNOLOGY

cessation experiments were conducted on B cells from Bcl-2-overexpressing mice. These cells proliferated and stopped, as for WT, but did not subsequently die confirming that regulation of division number is independent of the cellular machinery that leads to cell death (SI Fig. 9 *A* and *C*). Not all cells divide the same number of times and SI Fig. 9 illustrates how a truncated normal distribution provides an excellent fit to describe the variation in cell progression of a population of cells (Notes 12 and 13 in *SI Text*). Thus, the level of stimulation regulates the division number at which cells cease dividing. We shall refer to this number as a cell's "division destiny."

To accommodate the need to change cell division progression we implemented into GCytS the ability to vary the number of divisions taken by cells before they stop dividing by varying the progressor fractions, pF_i, for each division class. In accord with the above experiments we used a truncated normal distribution starting at division 1 (Note 14 in *SI Text*). This operation introduces two parameters, Dμ and Dσ, to describe the "division destiny" of cells or proportion that arrest in each division. Our implementation also assumes that division destiny is independent of times to first division (Note 13 in *SI Text*). This modified model was fitted to data for total cell number and cells per division from cell cessation experiments on WT cells (Fig. 4 *D–G*). Optimal solutions revealed that increasing the stimulation duration increased the Dμ value of division destiny (Fig. 4*H*). The modified GCytS could fit total cell number (Fig. 4 *D–G*) and cell number per division data (SI Fig. 10) from continuous and limited stimulation conditions extremely well. The rate of cell death in subsequent divisions found by GCytS fitting was consistent with lognormal probability densities of similar parameters for all stimulation conditions (Fig. 4*I*). Thus, the basic assumptions of the generalized cyton model including modulation of total division number apply extremely well to these complex experiments. When the modified GCytS was used to refit the data presented in Fig. 3 it detected a progressive dropping from cycle with division number and gave faster division times consistent with those reported in Fig. 4*I*. The reanalysis result is given in SI Fig. 11.

We envisage other scenarios are possible where parameter values will change with division. Such changes could be by means of internal division-linked programming, as seen for differentiation (29, 30), or they could be imposed from external signals by means of interactions with cells or exposure to cytokines. From a modeling perspective both internal and external regulation of the parameters can be treated in the same manner.

Quantitative Immune Responses. A period of antigen driven lymphocyte expansion *in vivo* is followed by cell death and contraction leaving a long-lived memory population (31, 32). This pattern of response is similar to that described above for cells following general cyton rules. That is the primary stimulus induces continued proliferation through a large number of divisions. Eventual cessation of proliferation triggering because of either internal limitations or external withdrawal of growth factors would lead to cell loss conforming to the underlying probabilistically distributed time to die in the expanded population. The typically long tail of a lognormal probability density function has the consequence that most cells die off whereas a proportion of cells can be left as long-lived, and potentially therefore serving as memory cells, without any explicit "programming" for longevity.

In SI Fig. 12 the cyton model is applied to *in vivo* data for the expansion, cessation of proliferation and subsequent death of CD8 and CD4 epitope-specific T cells in an LCMV infection (33). Analysis of these data illustrates the general application of our modeling approach. The data follows the cyton model encompassing the expansion phase and the 10- to 30-fold reduction in cell number before mechanisms for maintaining memory cell number take over. This mechanism could be differentiation to long lived memory cells or maintenance through homeostatic proliferation (34). Thus, whilst acknowledging that differentiation to memory
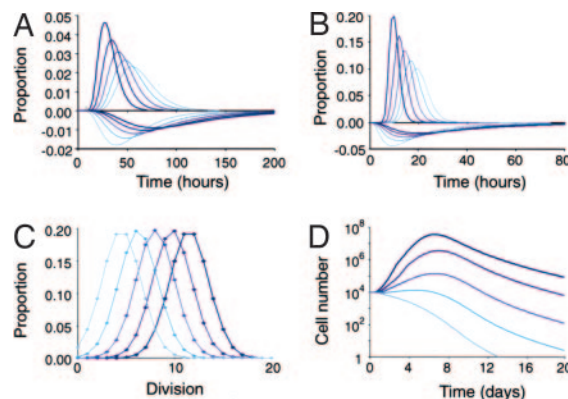

Fig. 5. Regulating adaptive immunity. This figure exemplifies the proliferation curves that result from varying parameters known to be affected by signal strength and by external signal regulation such as cytokines. (*A–C*) Parameters altered are the means of times to division and death (*A* and *B*) and the average number of divisions undergone (*C*). Parameter values varied at equally spaced intervals from: (*A*) ϕ_0 med = 30 h (darkest) to 60 h (lightest), s constant at 0.3 h and $\psi_{i>0}$ from 100 h to 50 h, s constant at 0.5 h; (*B*) $\phi_{i>0}$ from 10 h to 20 h, s constant at 0.2 h and $\psi_{i>0}$ from 35 h to 16 h, s constant at 0.75. pF_0 was set to 1.0 in all cases. Average division number (*C*) was defined by varying the mean of the division destiny distribution from Dμ = 12 (darkest) to Dμ = 5 (lightest), while keeping Dσ constant at 2. Possible outcomes are shown in *D*.

cells and acquisition of sensitivity to regulatory cytokines necessary for survival occurs *in vivo* (35), we suggest that the cyton rules of proliferation, cessation and loss still underlie the basic processes of the adaptive immune response.

Fig. 5 shows the family of patterns of adaptive response possible with different parameter values of the generalized cyton model. The parameters altered are those known to be influenced by signals: the means of times to divide and die and the distribution of division destiny. The figure emphasizes the quantitative nature of the immune response and how changes in parameter values can profoundly affect the outcome. Thus, we can ask, what regulates the eventual path? Clearly from the above discussion and previous work, lymphocyte subsets have different programmed outcomes for the number of divisions, rate of division and subsequent death rate (26, 28, 36). This outcome can be envisaged as a default response. However, further regulation through receptor delivered signals can alter this response. Cytokines, for example, can act on the division times, number of divisions and possibly variance of these values. In this way a default response in which cells are activated and proliferate but subsequently die away leading to clonal deletion can be converted progressively to one of weak positive outcome, to a strongly positive response with memory (Fig. 5*D*) by signals that reduce times to divide, increase times to die and increase the eventual number of divisions. A conceptual framework where the kinetic features of the immune response are triggered along a default path that can be modulated by additional regulatory signals may be useful as a basis for immune system modeling where the fate of each individual need not be determined.

Discussion

We have formulated a model of cell growth, cessation and death built on experimental evidence of how B cells interleave times to divide and die under different conditions. We believe our model is superior to alternatives such as the Smith–Martin-based models (10–14) or Deenick *et al*. models (7) and offers a general tool for examining regulation of growth and survival that is especially suited to data obtained from CFSE division tracking methods. Whereas formulated and tested here for B cells, the model is equally well applied to T cells and other regulated cell systems. Our model envisages the cell as comprising independent stochastic machines

controlling times to divide and die and the number of divisions possible. By incorporating independent variation associated with each machine a large number of alternative cell fates are realized and, surprisingly, the essential features of the adaptive immune response emerge

The cyton model was developed by taking a top-down view of the lymphocyte and asking what internal mechanisms must be operating to explain our quantitative data. We conclude that independent stochastic machinery governing cell division and death times are essential. Much is known of the molecular machinery governing cell division and death and the nature of signaling paths that modulate them (20, 37). Strikingly, the regulation requires sets of molecules that interact with each other, often through chains of enzyme-substrate interactions. The concentration and expression level of key molecules contribute to the timing of the regulated event (as is well illustrated for pro- and antiapoptotic molecules). Thus, the mechanism of timing the outcome can be understood. It is also possible to speculate as to the source of the variation. It is clear that protein products such as Bcl-2 are usually limiting for cell survival as overexpression extends lifespan in many cell types. Therefore, transcriptional variation intrinsic to expression of any protein (38, 39) will alter the lifetime of otherwise identical cells. Chains of interacting proteins each with transcriptional "errors" will contribute to further variance. Thus, there is ample explanation for the source of the variation. These complex internal processes, involving links of enzymes and limiting substrates, are also consistent with the class of skew probability distributions that fit the observed variation in timed events. The lognormal distribution is typically generated by a large number of sequential multiplicative events not unlike enzyme-product sequences. The gamma distribution arises from a series of consecutive stochastic events. It is tempting to suggest that the surprisingly large number of internal regulatory proteins found to control division and death has evolved partly to modulate time variation and adjust it to an appropriate range. If internal complexity has evolved to contribute a measured degree of stochasticity to cellular processes an important validating principle can be observed: When modeling complex cellular events an appropriate probability distribution can formally capture the intent of the myriad internal cellular processes governing the eventual outcome, without having to understand, or identify, each one (Note 15 in *SI Text*).

A key question that arises from our discussion therefore is whether the cellular division and death machinery is inevitably noisy, and inefficient, or whether it is deliberately so, as we argue here. Perhaps the system has evolved the complex number of links, regulators and epigenetic changes to allow the variance to reach an optimal level. This proposal would explain why cell cycle time variation is such a striking characteristic of cell growth (1–6).

Materials and Methods

Mice. Male C57BL/6 inbred mice were used for experiments. These animals were bred at the Walter and Eliza Hall Institute (WEHI) animal facility (Kew, Victoria, Australia) and were maintained in specific pathogen-free conditions at WEHI (Parkville) in accordance with institutional animal ethics committee regulations. Bcl-2 Vav and Bim KO mice were kindly provided by Alan Harris and Philippe Bouillet and also maintained at WEHI (Parkville).

Reagents and Antibodies. Recombinant mouse IL-4 was a gift of R. Kastelein (DNAX Research Institute, Palo Alto, CA). The α-CD40 antibody (1c10) was prepared from the original hybridoma (40) provided by DNAX Research Institute.

B Cell Isolation and Cell Culture. Single-cell suspensions were prepared from spleens and lymph nodes of mice, and red cells were lysed and run on discontinuous Percoll density gradients as described (41). Small dense cells were harvested from the 65%/80% interface, and B cells were purified by means of negative selection by using magnetic beads (Miltenyi Biotec, Bergisch Gladbach, Germany). For division tracking experiments, cells were labeled with CFSE (Molecular Probes, Eugene, OR) according to the originally published method (42). B cells were >95% B220$^+$, CD19$^+$, IgM$^+$, IgD$^+$ as determined by flow cytometry. B cells were cultured in B cell medium described in ref. 30. For stimulus withdrawal experiments, cells were precultured in stimulus for a designated time period before being washed twice in 37°C B cell medium and returned to culture.

Colcemid Analysis. For direct analysis of time of entry into first division, methodology defined in ref. 7 was followed.

Quantitative Implementation Method. A full description of the quantitative implementation method is in *SI Text*.

1. Cantrell DA, Smith KA (1984) *Science* 224:1312–1316.
2. Smith JA, Martin L (1973) *Proc Natl Acad Sci USA* 70:1263–1267.
3. Froese G (1964) *Exp Cell Res* 35:415–419.
4. Staudte RG, Guiguet M, d'Hooghe MC (1984) *J Theor Biol* 109, 127–46.
5. Dawson KB, Madoc-Jones H, Field EO (1965) *Exp Cell Res* 38:75–84.
6. Castor LN (1980) *Nature* 287:857–859.
7. Deenick EK, Gett AV, Hodgkin PD (2003) *J Immunol* 170:4963–4972.
8. Tangye SG, Avery DT, Deenick EK, Hodgkin PD (2003) *J Immunol* 170:686–694.
9. Gett AV, Hodgkin PD (2000) *Nat Immunol* 1:239–244.
10. De Boer RJ, Perelson AS (2005) *J Comp Appl Math* 184:104–164.
11. Ganusov VV, Pilyugin SS, de Boer RJ, Murali-Krishna K, Ahmed R, Antia R (2005) *J Immunol Methods* 298:183–200.
12. Leon K, Faro J, Carneiro J (2004) *J Theor Biol* 229:455–476.
13. Pilyugin SS, Ganusov VV, Murali-Krishna K, Ahmed R, Antia R (2003) *J Theor Biol* 225:275–283.
14. De Boer RJ, Ganusov VV, Milutinovic D, Hodgkin PD, Perelson AS (2006) *Bull Math Biol* 68:1011–1031.
15. Strasser A, Harris AW, Cory S (1991) *Cell* 67:889–899.
16. Wurster AL, Rodgers VL, White MF, Rothstein TL, Grusby MJ (2002) *J Biol Chem* 277:27169–27175.
17. Alderson MR, Pike BL, Nossal GJ (1987) *Proc Natl Acad Sci USA* 84:1389–1393.
18. Hudak SA, Gollnick SO, Conrad DH, Kehry MR (1987) *Proc Natl Acad Sci USA* 84:4606–4610.
19. Bouillet P, Metcalf D, Huang DC, Tarlinton DM, Kay TW, Kontgen F, Adams JM, Strasser A (1999) *Science* 286:1735–1738.
20. Cory S, Huang DC, Adams JM (2003) *Oncogene* 22:8590–8607.
21. Hasbold J, Hong JS, Kehry MR, Hodgkin PD (1999) *J Immunol* 163:4175–4181.
22. Shields R (1977) *Nature* 267:704–707.
23. Pereira JP, Girard R, Chaby R, Cumano A, Vieira P (2003) *Nat Immunol* 4:464–470.
24. Akaike H (1973) in *Proceedings of the Second International Symposium on Information Theory*, eds Petrov BN and Caski F (Akadémiai Kiadó, Budapest), pp 267–281.
25. Burnham KP, Anderson DR (2002) *Model Selection and Multimodel Inference: A Practical Information-Theoretic Approach* (Springer–Verlag, New York).
26. Rush JS, Hodgkin PD (2001) *Eur J Immunol* 31:1150–1159.
27. van Stipdonk MJ, Hardenberg G, Bijker MS, Lemmens EE, Droin NM, Green DR, Schoenberger SP (2003) *Nat Immunol* 4:361–365.
28. Kaech SM, Ahmed R (2001) *Nat Immunol* 2:415–422.
29. Hodgkin PD, Lee JH, Lyons AB (1996) *J Exp Med* 184:277–281.
30. Hasbold J, Corcoran LM, Tarlinton DM, Tangye SG, Hodgkin PD (2004) *Nat Immunol* 5:55–63.
31. Murali-Krishna K, Altman JD, Suresh M, Sourdive D, Zajac A, Ahmed R (1998) *Adv Exp Med Biol* 452:123–142.
32. McDonnell TJ, Deane N, Platt FM, Nunez G, Jaeger U, McKearn JP, Korsmeyer SJ (1989) *Cell* 57:79–88.
33. Homann D, Teyton L, Oldstone MB (2001) *Nat Med* 7:913–919.
34. De Boer RJ, Homann D, Perelson AS (2003) *J Immunol* 171:3928–3935.
35. Gourley TS, Wherry EJ, Masopust D, Ahmed R (2004) *Semin Immunol* 16:323–333.
36. Murali-Krishna K, Altman JD, Suresh M, Sourdive DJ, Zajac AJ, Miller JD, Slansky J, Ahmed R (1998) *Immunity* 8:177–187.
37. Nurse P (2000) *Cell* 100:71–78.
38. Hume DA (2000) *Blood* 96:2323–2328.
39. Kaern M, Elston TC, Blake WJ, Collins JJ (2005) *Nat Rev Genet* 6:451–464.
40. Heath AW, Wu WW, Howard MC (1994) *Eur J Immunol* 24:1828–1834.
41. Deenick EK, Hasbold J, Hodgkin PD (1999) *J Immunol* 163:4707–4714.
42. Lyons AB, Parish CR (1994) *J Immunol Methods* 171:131–137.

IMMUNOLOGY